Journal of Inorganic and General Chemistry
ZAAC
Zeitschrift für anorganische und allgemeine Chemie
DOI: 10.1002/zaac.202100092
ARTICLE

Stable, but still reactive – investigations on the effects of Lewis acid binding on copper nitrene intermediates

Katrin Warm[+],[a] Inés Monte Pérez[+],[a] Uwe Kuhlmann,[b] Peter Hildebrandt,[b] Erik Farquhar,[c] Marcel Swart,*[d] and Kallol Ray*[a]

Copper nitrenes are proposed as reactive intermediates in a number of copper mediated aziridination and amination reactions. However, the isolation and characterization of such intermediates have proved challenging because of their transient nature. One successful approach for the stabilization of the copper-nitrene cores is the employment of a redox innocent Lewis acid (LA) like Sc^{3+}. We herein report the stabilization of two transient copper nitrene species **3** and **4** in the absence of LAs by employing electronegative $-CF_3$ and $-NO_2$ groups in the nitrene substituent. Detailed investigations of the spectroscopic properties of **3** and **4** by theoretical and experimental methods, and a comparison of their reactivities in presence and absence of LAs provide some vital insights into the effect of LAs on the geometric and electronic structures of the copper nitrenes.

Introduction

Nature employs metalloenzymes as biocatalysts for a variety of small molecule activation reactions. In many enzyme-catalyzed oxidation reactions, the metal ions in the reactive centers traverse highly reactive intermediate high-valent oxidation states. For example, the potent oxidants responsible for the activation of C–H bonds in Cu-containing monooxygenases like the particulate methane monooxygenase (pMMO) and other hydroxylating Cu-enzymes are believed to be Cu(II)-oxyl species;[1] however, despite extensive synthetic efforts these species have remained elusive to the synthetic bioinorganic community. In some rare cases, however, $[Cu(O)]^+$ cores could be trapped in the gas-phase.[2]

Terminal Cu-nitrene complexes, which are isolectronic to copper-oxo, have also eluded detection for decades, although they are proposed as reactive intermediates in various copper mediated amination and aziridination reactions. Warren and co-workers indirectly proposed the involvement of terminal copper–nitrene intermediates derived from dicopper–nitrene species by NMR exchange experiments and kinetic measurements of C–H functionalization reactions.[3a,b] Furthermore, Bertrand and co-workers provided evidence of copper(II)–bis(nitrene) and dicopper(II)–nitrene species in solution based on ^{31}P NMR studies.[3c] Isolation and spectroscopic characterization of terminal copper nitrene cores were, however, not possible, until very recently.[3d–j] The first copper nitrene complex $[(AN)Cu(NTs)Sc(OTf)_3]^+$ **1-Sc** (AN = 3,3′-iminobis(N,N-dimethylpropylamine, Ts = *p*-tolylsulfonyl) could be trapped in our group[3e] by applying the stabilizing effect of a Lewis acid (LA) like $Sc(OTf)_3$ (Scheme 1), a strategy that has also been employed previously for the stabilization of the transient metal oxo cores of Fe, Co and Ni.[4] The demonstrated abilities of **1-Sc** to perform C–H abstraction and nitrene transfer reactions are consistent with the proposed involvement[3h,5] of copper-nitrenes as reactive intermediates in various amination and aziridination reactions. Detailed spectroscopic characterization of **1-Sc** revealed that its electronic configuration is best described as a copper(II) nitrene radical complex with a singlet ground state.[3e] Further studies on the role of the Lewis acid showed a correlation between the Lewis acid strength and the observed yield of the copper nitrene complexes **1-M** ($M=Sc^{3+}$, Y^{3+}, Eu^{3+}, Ce^{3+}, Zn^{2+}, Ca^{2+}).[3d] In addition, a two-state reactivity model, well established in the metal-oxo chemistry,[6] is also shown to be applicable for controlling the reactivity of the copper nitrenes. A comparison of the reactivity of **1-Sc** and $[(AN)Cu(NMes)Sc(OTf)_3]^+$ (**2-Sc**, Mes = mesityl) in a follow-up study established the former as a stronger hydrogen atom transfer (HAT) and a weaker nitrene transfer (NT) agent than **2-**

[a] *K. Warm,[+] Dr. I. Monte Pérez,[+] Prof. Dr. K. Ray*
Institut für Chemie
Humboldt-Universität zu Berlin
Brook-Taylor-Straße 2, 12489 Berlin, Germany
E-mail: kallol.ray@hu-berlin.de
[b] *Dr. U. Kuhlmann, Prof. Dr. P. Hildebrandt*
Institut für Chemie
Technische Universität Berlin
Fakultät II
Straße des 17. Juni 135, 10623 Berlin, Germany
[c] *Dr. E. Farquhar*
Brookhaven National Laboratory
NSLS-II, Bldg. 745, Room 106, P.O. Box 5000,
11973-5000 Upton, NY, United States
[d] *Prof. Dr. M. Swart*
Institut de Química Computacional i Catàlisi
Universitat de Girona, Campus Montilivi (Ciències)
Maria Aurèlia Capmany i Farnés, 69, 17003 Girona, ICREA and
Pg. Lluís Companys 23, 08010 Barcelona, Spain
E-mail: marcel.swart@udg.edu
[+] *equal contribution of the two authors*

Supporting information for this article is available on the WWW under https://doi.org/10.1002/zaac.202100092

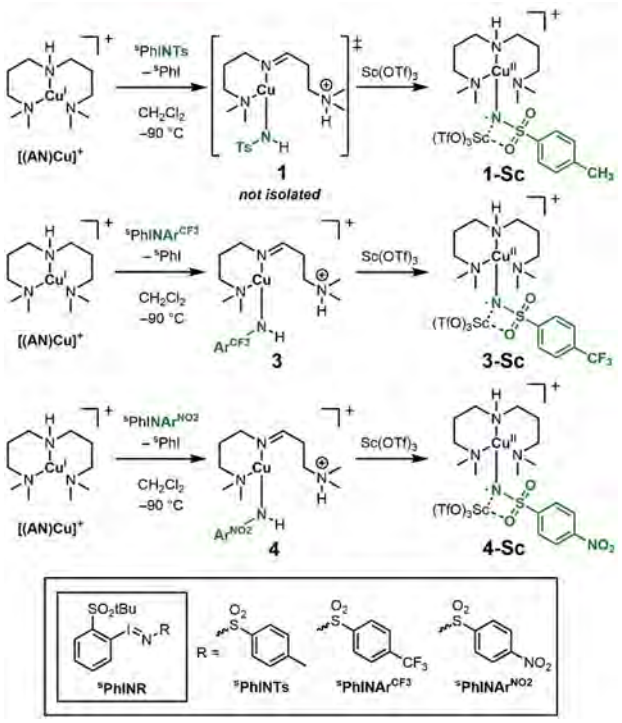

Scheme 1. Schematic overview of the complexes investigated in the present study.

Sc. This contrasting reactivity trend in HAT and NT reactions was attributed to the easier access of the excited $S=1$ state in **1-Sc**, but not in **2-Sc**.[3f] Examples of copper-nitrene complexes in the triplet ground state have also been reported;[3g–i] one recent highlight is the X-ray crystal structure of a $[Cu^{I}(^{3}NR)]^{+}$ core containing a triplet nitrene group attached to a central Cu(I) center.[3i] These complexes are, however, sluggish oxidants; their attenuated reactivity, in spite of the stabilization of the more reactive $S=1$ state, has been attributed to the steric profiles of the ancillary ligands.

In the present study we report the stabilization of the two new copper nitrene complexes [(AN)Cu(NAr^{CF3})]; (**3**; $Ar^{CF3}=p$-trifluoromethylphenylsulfonyl) and [(AN)Cu(NAr^{NO2})] (**4**; $Ar^{NO2}=p$-nitrophenylsulfonyl), where the introduction of the electron-withdrawing $-CF_3$ and $-NO_2$ groups into the nitrene substituent enabled us to stabilize the previously reported $S=0$ Cu^{II}-NR· core in the absence of any externally added LAs (Scheme 1). A detailed investigation of the spectroscopic and reactivity properties of **3** and **4**, as well as their LA-adducts, **3-Sc** and **4-Sc**, by experimental and theoretical methods, provides some new insights into the reactivity and the geometric and electronic structures of the copper nitrene core.

Results and Discussion

In an effort to evaluate the electronic effect of the nitrene substituents on the copper nitrene cores, we aimed at the generation of the new copper nitrene intermediates bearing a close structural similarity to **1-Sc**. For our purpose, we employed the two derivatives of the previously used soluble nitrene source sPhINTs ([*N*-(*p*-toluenesulfonyl)imino](2-*tert*-butylsulfonyl) phenyliodinane), in which the $-CH_3$ group of the tosyl substituent was substituted by the electron-withdrawing $-CF_3$ (sPhINAr^{CF3}) or $-NO_2$ (sPhINAr^{NO2}) groups. The reaction of the Cu(I) precursor [(AN)Cu](BF_4) with sPhINAr^{CF3} or sPhINAr^{NO2} at $-90\,^{\circ}C$ in presence of $Sc(OTf)_3$ in CH_2Cl_2 yielded [(AN)Cu(NAr^{CF3})$Sc(OTf)_3]^{+}$ (**3-Sc**) and [(AN)Cu(NAr^{NO2})$Sc(OTf)_3]^{+}$ (**4-Sc**), respectively, with electronic absorption bands at 525 nm ($\varepsilon_{3\text{-}Sc}=2150\ M^{-1}cm^{-1}$; $\varepsilon_{4\text{-}Sc}=2000\ M^{-1}cm^{-1}$) and 750 nm ($\varepsilon_{3\text{-}Sc}=600\ M^{-1}cm^{-1}$; $\varepsilon_{4\text{-}Sc}=550\ M^{-1}cm^{-1}$), which slowly decayed with half-lives of 2250 s for **3-Sc** and 3000 s for **4-Sc** (Figure 1). Notably, the half-life of **1-Sc** was previously reported to be only 1600 s;[3b] the observed trend in the thermal stabilities (**1-Sc** < **3-Sc** < **4-Sc**) plausibly reflects the increasing electron withdrawing effects of the *p*-X-benzylsulfonyl nitrene substituent as X is varied from $-CH_3$ to $-CF_3$ and to $-NO_2$.

Interestingly, the electron-withdrawing effect of the $-CF_3$ and $-NO_2$ substituents also provided access to the [(AN)Cu(NAr^{CF3})]$^{+}$ (**3**) and [(AN)Cu(NAr^{NO2})]$^{+}$ (**4**) intermediates, in the reactions of [(AN)Cu](BF_4) with sPhINAr^{CF3} or sPhINAr^{NO2} in CH_2Cl_2 at $-90\,^{\circ}C$, without the addition of LAs. The UV-Vis spectra of **3** and **4** showed bands at 425 nm ($\varepsilon_3=1200\ M^{-1}cm^{-1}$; $\varepsilon_4=1300\ M^{-1}cm^{-1}$) and 700 nm ($\varepsilon_3=600\ M^{-1}cm^{-1}$; $\varepsilon_4=700\ M^{-1}cm^{-1}$) (Figure 1), which were significantly blue shifted relative to **3-Sc** and **4-Sc**. Titration experiments (Figure S1) revealed that 1 equiv. of sPhINAr^{NO2} is necessary for the maximum absorbance at 425 nm corresponding to **4**, which is consistent with the [(AN)Cu(NAr^{NO2})]$^{+}$ assignment. Half-lives of 1200 s and 1400 s were measured for **3** and **4**, respectively, at $-90\,^{\circ}C$. The higher thermal stability of **4** relative to **3**, and our inability to trap **1** in the absence of any LA, again reflect the trend of the increasing electron withdrawing effects of $NO_2 > CF_3 > CH_3$, thereby corroborating the proposed role of the LAs in the stabilization of the copper nitrenes.

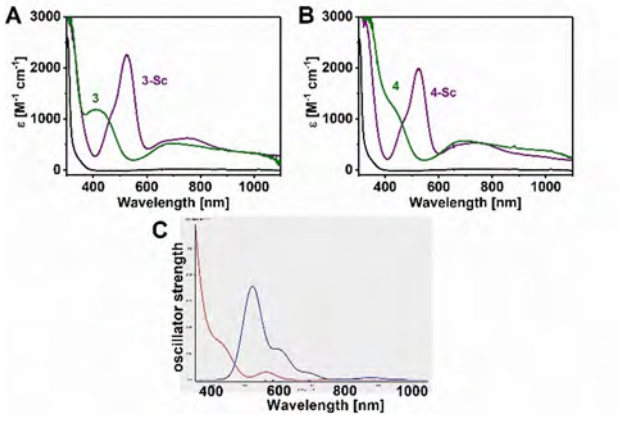

Figure 1. A) Absorption spectra of **3** (green) and **3-Sc** (purple) in CH_2Cl_2 at $-90\,^{\circ}C$; B) Absorption spectra of **4** (green) and **4-Sc** (purple) in CH_2Cl_2 at $-90\,^{\circ}C$; the initial [(AN)Cu](BF_4) absorption spectra are shown in black in each case; C) DFT calculated electronic absorption spectra for **4** (red) and **4-Sc** (blue).

3-Sc and **4-Sc** could be reduced to the corresponding copper(I) complexes by a one-electron reductant like ferrocene (Fc, E_{ox} vs SCE = 0.37 V) with the concomitant formation of ferrocenium (Fc^+) cation in 150–160% yield (Figure S2). This confirmed that **3-Sc** and **4-Sc** are two oxidation levels above [(AN)Cu](BF_4). Interestingly, complexes **3** and **4** could not oxidize Fc in the absence of any LAs; thus the binding of LAs results in a positive shift of the $[Cu(NR)]^{+/0}$ potential. All the four complexes could, however, be reduced to [(AN)Cu](BF_4) in presence of a stronger reductant like decamethylferrocene ($Me_{10}Fc$, E_{ox} vs SCE = −0.08 V) with the formation of $Me_{10}Fc^+$ in 187–193% yields (Figure S3). This is consistent with a formal Cu(III) assignment for **3**, **3-Sc**, **4** and **4-Sc**, with a yield of > 90% in each case.

Further insights into the oxidation state of the Cu ion were provided by X-ray absorption near edge structure (XANES) analysis of the Cu K-edge of **4** and **4-Sc**. Interestingly, both the intermediates display near identical XANES spectra, which shows that the immediate electronic environment of the Cu ion is independent of the Lewis acid binding. Comparison of the edge energies obtained for **4** and **4-Sc** to the Cu(I) precursor reveals a shift to higher energies upon oxidation (Figure 2A). The 1 s→3 d pre-edge transition found at ca. 8978 eV for both **4** and **4-Sc** suggests the presence of a Cu(II) centre in both cases. Based on the formal Cu(III) assignment and the XANES determined physical oxidation state of +2, the electronic structure in **4** and **4-Sc** can be best described as copper(II) nitrene radical (similar to **1-Sc**).

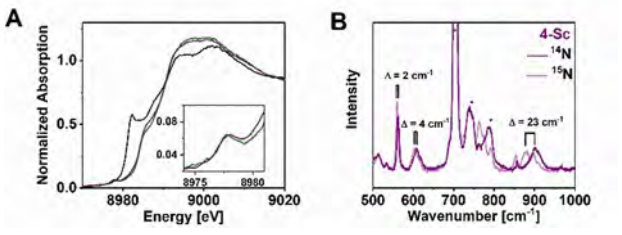

Figure 2. A) Normalized Cu K-edge spectra for [(AN)Cu](BF_4) (black), **4** (green) and **4-Sc** (purple) in frozen CH_2Cl_2 solutions; the inset shows a zoom on the pre-edge features of **4** and **4-Sc** around 8978 eV; B) rRaman spectra of **4-Sc** (purple) generated with ^{14}N-labelled (purple) ^{s}PhINAr^{CF3} and with ^{15}N-labelled (light purple) ^{s}PhINAr^{CF3} and measured with 532 nm laser excitation in a CH_2Cl_2/acetone mixture (20:1) at −90 °C.

Resonance Raman (rRaman) spectroscopy performed at −90 °C on **3-Sc** and **4-Sc** with 532 nm laser irradiation showed three $^{14/15}$N isotope-sensitive bands in each case (Figures 2B, S4). For **4-Sc** (Figure 2B) a vibration involving primarily the Cu–N bond was identified at 902 cm^{-1} on the basis of its shift ($^{15/14}\Delta\nu$) to lower wavenumbers by 23 cm^{-1} ($^{15/14}\Delta\nu_{calc.} = 25$ cm^{-1}) upon ^{15}N-labelling. For **3-Sc** this band is observed at 897 cm^{-1} with a $^{15/14}\Delta\nu_{exp.}$ of 24 cm^{-1}. Two further features at 608 and 562 cm^{-1} were found to shift by 2 cm^{-1} and 4 cm^{-1} upon ^{15}N labelling (for **3-Sc** the corresponding bands were observed at 609 and 558 cm^{-1}, respectively, with a $^{15/14}\Delta\nu_{exp.}$ of 2 cm^{-1} in each case). Unfortunately, the lower thermal stabilities of **3** and **4** prevented the acquisition of rRaman spectra for these intermediates.

The stabilization of the $[(AN)Cu(NAr^{CF3})]^+$ and $[(AN)Cu(NAr^{NO2})]^+$ cores in presence and absence of Sc^{3+}, provided us with a unique opportunity to investigate the role of Sc^{3+} in copper nitrene mediated HAT and NT reactions (Table 1). Interestingly, comparable second-order rates were obtained for the HAT reactions of **3** and **3-Sc** with toluene (Figure 3A, B; Figures S5,6). Similarly, the binding of Sc^{3+} had no significant effect on the reaction rates for complex **4** mediated HAT from toluene (Figures 3C, D; S5, S6) or NT (Figure S7) to thioanisole. Furthermore, the deuterium kinetic isotope effects (KIE) determined for the HAT reactions from xanthene and d_2-xanthene, respectively, for **4** (KIE = 4.4) and **4-Sc** (KIE = 4.3) can be considered as equal within the error of experimental measurements (Figure S8).

Thus, although the binding of Sc^{3+} results in a positive shift of the $[Cu(NR)]^{+/0}$ reduction potential, no effect has been observed on the HAT and NT reaction rates. This can be rationalized by assuming that the species responsible for the HAT and NT reactivities is the free copper nitrene, which is present in equilibrium with the Sc^{3+} adduct in solution (Scheme 2). The existence of this equilibrium is further corroborated by a systematic study of the reaction rates of **4-Sc** with 1,4-cyclohexadiene (CHD) in presence of different amounts of Sc^{3+}. Within the solubility limit of $Sc(OTf)_3$ a linear decrease of the rate constant k_2 with increasing amounts of $Sc(OTf)_3$ in solution could be observed (Figure S9). This supports the presence of an equilibrium in solution, as elevated amounts of Sc^{3+} shift the equilibrium towards the Sc^{3+} adduct and diminish the concentration of the free nitrene in solution, thereby accounting for the diminished reactivity.

Table 1. Second-order rate constants k_2 for the reactions of **1-Sc**, **3**, **3-Sc**, **4** and **4-Sc** with different substrates in CH_2Cl_2 at −90 °C.

Substrate (BDE_{C-H} [kcal/mol])	k_2 [$M^{-1}s^{-1}$] **1-Sc**[3b]	**3**	**3-Sc**	**4**	**4-Sc**
HAA					
Xanthene (75.2)	0.311(2)	nd	nd	0.105(1)	0.108(1)
CHD (76)	0.155(1)	nd	nd	0.061(2)	0.061(2)
Toluene (89.7)	0.0051(2)	0.0033(3)	0.0031(1)	0.0026(2)	0.0025(1)
NT					
Thioanisole	No rxn	nd	nd	0.110(2)	0.112(2)

nd = not determined.

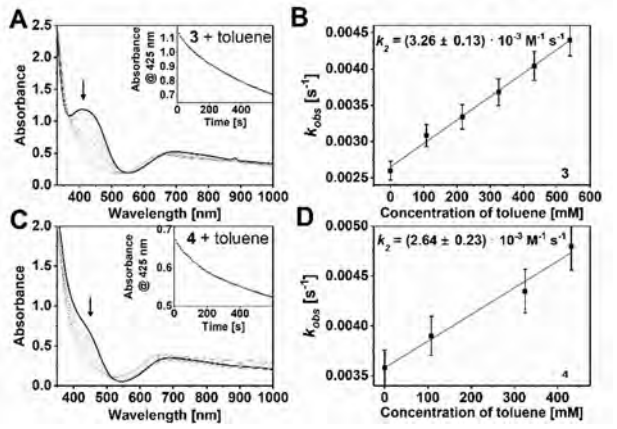

Figure 3. A) UV-Vis spectral changes upon the addition of toluene to a preformed solution of **3** in CH_2Cl_2 at −90 °C; inset shows the time trace of the decay of the 425 nm band; B) Plot of the pseudo-first order rate constants k_{obs} vs the substrate concentration for the reaction of **3** with toluene and a linear fit of the data to determine the second-order rate constant k_2; C) UV-Vis spectral changes upon the addition of toluene to a preformed solution of **4** in CH_2Cl_2 at −90 °C; inset shows the time trace of the decay of the 425 nm band; D) Plot of the pseudo-first order rate constants k_{obs} vs the substrate concentration for the reaction of **4** with toluene and a linear fit of the data to determine the second-order rate constant k_2.

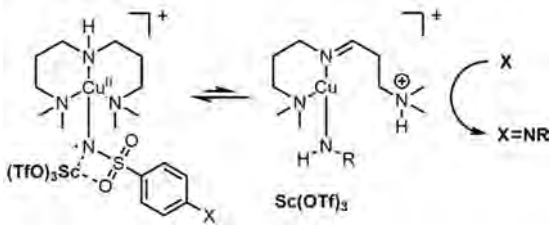

Scheme 2. Proposed equilibrium between the stabilized Lewis acid adduct and the reactive free copper nitrene species.

DFT calculations provided further insights into the geometric structures of the [(AN)Cu(NR)]$^+$ and [(AN)Cu(NR)(Sc(OTf)$_3$)]$^+$ complexes. Unlike the previous study where the Sc-triflate moiety was approximated by a ScF_3 ligand,[3b] here we used the full structure of the scandium triflate moiety [Sc(OTf)$_3$]. For the structure of [(AN)Cu(NR)(Sc(OTf)$_3$)]$^+$, a number of different conformations for both the tosyl moiety and each of the triflate groups were sampled, leading to two major conformers **A** and **B** as shown in Figure 4 (Figure S10). In conformer **B** one of the tosyl oxygens has a weak coordination towards copper with a Cu–O distance of 2.41 Å (thereby resulting in a five coordinate (5 C) Cu), as reported previously, while this weak coordination is absent in conformer **A**. Instead, in conformer **A** the other tosyl oxygen is coordinating to the scandium with a Sc–O distance of 2.20 Å. In our calculations, conformer **A** is always found to be stable (Table S3), irrespective of the nature of the *para*-substituent (CH_3, CF_3 or NO_2). This is also consistent with the expected higher oxophilicity of Sc^{3+} ion relative to Cu^{2+}.

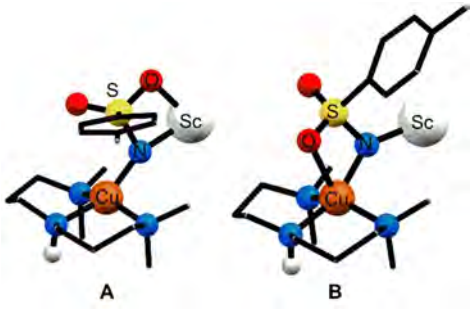

Figure 4. Coordination environment of the Cu nitrene unit in **1-Sc** in conformations **A** (left) and **B** (right); Sc-bound triflate counterions are omitted for clarity (Cu: orange, N: blue, S: yellow, O: red, Sc: big white, H: small white balls); for the complete structures and the relative energies of the conformers, see Figure S10 and Table S3.

The preference for conformer **A** is also corroborated by calculation of the UV-Vis spectra for both the conformers. Experimentally, a single band had been observed in the visible region around ca. 525 nm (Figure 1). Figure S11 shows the calculated spectra for both the conformers **A** and **B**, where a single band around 520 nm is obtained for conformer **A** (Figure 1C). For conformer **B**, on the other hand, two bands at ca. 860 nm and 575 nm with a shoulder at ca. 520 nm (Figure S11) were observed, which are inconsistent with the experiment. Therefore, both the UV-Vis spectra and the DFT stabilization energies clearly indicate that conformer **A** is the most probable structure of the [(AN)Cu(NR)(Sc(OTf$_3$)]$^+$ complexes .

We now move on to the effect that the different Lewis acids may have on the UV-Vis spectra of the [(AN)Cu(NR)(M(OTf)$_3$)]$^+$ (**1-M**; M=Sc^{3+}, Y^{3+}, Eu^{3+}, Ce^{3+}, Zn^{2+}, Ca^{2+}) complexes. Previously, it was shown experimentally for **1-M** complexes that both the peak position and the intensity of the band at ca. 525 nm were independent of the nature of LAs.[3a] Given the different expected coordinations of e.g. divalent Zn/Ca vs. trivalent Sc/Y, it was unclear why the observed UV-Vis spectra were so similar (Figure S12, Table S1). Therefore, we expanded our density functional study by including the species with the different LAs. For all the **1-M** complexes conformation **A** is energetically stable irrespective of the nature of M. The resulting UV-Vis absorption spectra for the four Lewis-acid stabilized copper nitrenes are shown in the Figure S13 in the most stable conformation **A**. The origin for the lack of change in the UV/Vis spectra when changing the LAs became immediately clear by looking at the transitions involved in the UV/vis peak at ca. 520–530 nm. For instance for the [Sc(OTf$_3$)] stabilized copper nitrene in conformation **A**, the peak at 527 nm results from two main transitions: 36% 224α→232α and 37% 228α→232α (see Figure S14). As can be observed from this figure, the occupied 224α and 228α orbitals are mainly located at the tosyl group and the ancillary AN ligand, while the virtual 232α orbital is located mainly on copper and the AN ligand (and on the

nitrene).Thus this transition is predominantly ligand to metal charge transfer in origin; the observed blue shift of this band in the absence of LAs is in agreement with the reduction in the $[Cu(NR)]^{+/0}$ reduction potential. Similar transitions have been observed for the other Lewis-acid stabilized complexes. Hence, since the molecular orbitals involved in the transition that is responsible for the 525 nm peak do not contain any (major) contribution from the Lewis-acid moiety, the effect of which kind of Lewis-acid is present does not affect these transitions.

What remains to be determined is the structure of the copper nitrene without the Lewis-acid present. A number of possible coordination modes could be envisioned, among which the simplest one is to have the $[Sc(OTf)_3]$ stabilized structure (conformation **A**) and simply removing the Lewis acid moiety (the so-called "LA-remove" conformation, Figures 5/S15, left). In another possibility, one of the amine groups of the AN ligand drifts away and the nitrene group is protonated instead of the middle amine group (the so-called "diamine" conformation, Figures 5/S15, middle). The most stable structure (Figures 5/S15 right) is similar to the "diamine" conformation, and also features a protonated amine group, and a bidentate binding mode of the AN ligand. However, surprisingly, during the geometry optimization the far-away amine group deprotonates a CH_2 group next to the middle amine group, thereby forming an imine in the middle and an ammonium cation on the side (see Figures 5/S15 right). This new structure is ca. 35 kcal·mol^{-1} more stable than the "LA-remove" conformation. Moreover, the computed UV/vis spectra for this species is in reasonable agreement with the experimentally observed spectrum (Figure 1C).[7] Therefore, similar to what was already shown for the Lewis-acid stabilized complexes, there is a direct match between the most stable structure and the computed UV/vis absorption spectra that agrees well with the experiment in both cases (Figure 1C, Table S2).

Conclusions

In summary, detailed theoretical studies have provided new insights into the geometric structure of the previously reported LA stabilized $[(AN)Cu(NR)]^+$ complexes. In the presence of externally added redox non-innocent M^{n+} ions, the $[(AN)Cu^{II}(NR\cdot)(M(OTf)_3)]^+$ complexes in the open-shell singlet state are stabilized in conformation **A**, where one of the tosyl oxygens binds to the M^{n+} ions and the Cu^{2+} ion stays 4 C. The previously suggested[3b] conformation **B** with a 5 C Cu^{2+} ion is not consistent with the higher oxophilicity of the M^{n+} ions as well as the experimental UV/Vis spectra with a strong band at 525 nm. The characteristic 525 nm band is predominantly nitrene to Cu charge transfer in character; its transition energy is found to be independent of the nature of the M^{n+} ions in both the experimental and the theoretically calculated spectra. The stabilizing effect of the LAs can also be replaced by the introduction of the electron withdrawing $-NO_2$ and $-CF_3$ groups in the nitrene substituent, which has enabled the stabilization of **3** and **4** even in the absence of LAs. However, a structural reorganization occurs, whereby the Cu^{2+} becomes 3 C along with the deprotonation of the central amine nitrogen and the concomitant protonation of the nitrene- and one of the terminal amines. The binding of the M^{n+} ions has significant influence on the $[Cu(NR)]^{+/0}$ reduction potential and also on the thermodynamic stability of the copper-nitrene core. A trend of increasing Cu–N stretching frequencies from 843 cm^{-1} in **1-Sc** to 897 cm^{-1} in **3-Sc** and to 902 cm^{-1} in **4-Sc** follows the increasing electron-withdrawing effect of the tosyl *p*-substituent in the order $NO_2 > CF_3 > CH_3$. Surprisingly, however, the presence or absence of LAs made no difference on the observed reaction rates for the copper-nitrene mediated HAT and NT reactions. This reveals that the bare copper nitrene intermediate in both cases is responsible for the observed reactivities.

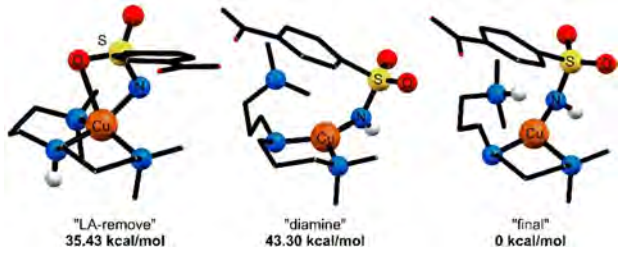

Figure 5. DFT calculated possible structures of the bare Cu nitrene unit in the "LA-remove" (left), the "diamine" (middle) and the "final most stable" (right) conformations;); Only selected H-atoms are shown for clarity (Cu: orange, N: blue, S: yellow, O: red, H: white).

Experimental Section

Experimental Details. All the chemicals were purchased and used directly. $[(AN)Cu](BF_4)$, and 2-(*tert*-butylsulfonyl)(diacetoxyiodo) benzene (^{s}PhI(OAc)$_2$) were synthesized following previous reports.[3b,8] Preparation and handling of air-sensitive samples were performed in a N_2-filled glovebox OMNI-Lab 2 (VAC) with O_2 and moisture concentrations <1 ppm or maintaining an inert atmosphere using Schlenk techniques. UV-Vis spectra were recorded with an Agilent 8453 diode array spectrometer equipped with a cryostat from Unisoku Scientific Instruments, Japan.

Synthesis of the oxidant ^{s}PhINAr^{CF3}: 4-(trifluoromethyl) benzenesulfonamide (0.15 g, 0.68 mmol)) and potassium hydroxide (0.10 g, 1.70 mmol) were dissolved in 5 mL methanol. The resultant solution was stirred in an ice bath at 0 °C for 15 minutes. After this time ^{s}PhI(OAc)$_2$ (0.30 g, 0.68 mmol) was slowly added. The reaction mixture was kept stirring at 0 °C for 1 hour and then at room temperature for 2 hours. The white suspension thus obtained was poured to crashed ice and this mixture was filtrated before the ice was completely melted. The white residue was washed with water until neutral pH and then with Et_2O. After drying under vacuum overnight, the oxidant ^{s}PhINAr^{CF3} was obtained as a white solid (0.214 g, 0.39 mmol, 58 %). ^{1}H NMR (CD_2Cl_2, 300 MHz): $\delta = 8.11$ (d, 1H, *H*-Ar), 8.01 (d, 2H, *H*-Ar), 7.92 (d, 1H, *H*-Ar), 7.81 (t, 1H, *H*-Ar), 7.73 (d, 1H, *H*-Ar), 7.68 (d, 3H, *H*-Ar), 1.42 (s, 9H, $C(CH_3)_3$); ^{13}C NMR (CD_2Cl_2, 101 MHz) $\delta = 149.0$ (C_{Ar}-SO_2N), 137.5 (C_{Ar}-H), 135.2 (C_{Ar}-H), 133.4 (C_{Ar}-SO_2tBu), 132.5 (C_{Ar}-H), 129.3 (C_{Ar}-H), 128.5 (C_{Ar}-H), 127.3 (q, $J = 3.6$ Hz, CF_3), 116.1 (C_{Ar}-I), 65.0 ($C(CH_3)_3$), 24.5 (CH_3); ESI-MS (+): $m/z = 569.950$ $[C_{17}H_{17}F_3INO_4S_2 + Na]^+$ (calc. 569.949).

For the preparation of the labelled ^{s}PhI^{15}NAr^{CF3} the same procedure was performed using ^{15}N-4-(trifluoromethyl)benzenesulfonamide. ESI-MS (+): $m/z = 570.952$ $[C_{17}H_{17}F_3I^{15}NO_4S_2 + Na]^+$ (calc. 570.946).

Synthesis of the oxidant ^{s}PhINAr^{NO2}: 4-nitrobenzenesulfonamide (0.14 g, 0.68 mmol) and potassium hydroxide (0.10 g, 1.70 mmol) were dissolved in 4 mL methanol. The resultant solution was stirred in an ice bath at 0 °C for 15 minutes. After this time ^{s}PhI(OAc)$_2$ (0.30 g, 0.68 mmol) was slowly added. The reaction mixture was kept stirring at 0 °C for 1 hour and then at room temperature for 2 hours. The white suspension thus obtained was poured to crashed ice and this mixture was filtrated before the ice was completely melted. The white residue was washed with water until neutral pH and then with Et_2O. Drying in vacuum overnight yielded the oxidant ^{s}PhINAr^{NO2} as white solid (0.284 g, 0.23 mmol, 80 %). ^{1}H NMR (CD_2Cl_2, 300 MHz): $\delta = 8.26$ (d, 1H, *H*-Ar), 8.19 (d, 1H, *H*-Ar), 8.06 (d, 1H, *H*-Ar), 7.94 (dd, 1H, *H*-Ar), 7.87 (td, 1H, *H*-Ar), 7.75 (td, 2H, *H*-Ar), 1.44 (s, 9H, $C(CH_3)_3$); ESI-MS (+): $m/z = 546.946$ $[C_{16}H_{17}IN_2O_6S_2 + Na]^+$ (calc. 546.947); AT-IR (solid): ν [cm^{-1}] = 1518 (s), 1474 (m), 1443 (m), 1425 (m), 1346 (s), 1290 (s), 1263 (s), 1166 (m), 1146 (w), 1137 (w), 1124 (s), 1108 (m), 1077 (s), 1010 (m), 1001 (m), ***877*** (s), ***851*** (s), 779 (m), 733 (s), 698 (w), 687 (m), 650 (s), 569 (s), 549 (s), 516 (m), 464 (s).

For the preparation of the labelled ^{s}PhI^{15}NAr^{NO2} the same procedure was performed using ^{15}N-4-nitrobenzenesulfonamide. ESI-MS (+): $m/z = 547.950$ $[C_{16}H_{17}IN^{15}NO_6S_2 + Na]^+$ (calc. 547.944); AT-IR (solid): ν [cm^{-1}] = 1518 (s), 1474 (m), 1443 (m), 1425 (m), 1346 (s), 1290 (s), 1263 (s), 1166 (m), 1146 (w), 1137 (w), 1124 (s), 1108 (m), 1077 (s), 1010 (m), 1001 (m), ***865*** (s), ***845*** (s), 779 (m), 733 (s), 698 (w), 687 (m), 642 (s), 569 (s), 549 (s), 516 (m), 464 (s).

General procedure for the generation of 3-Sc and 4-Sc: Under inert conditions, a colourless solution of the complex [(AN)Cu](BF$_4$) in anhydrous CH_2Cl_2 (1 mM, 2 mL) was cooled down to −90 °C. Then 1.5 equivalents of the Lewis acid (Sc(OTf)$_3$) in anhydrous acetone (0.1 mL) and 1.5 equivalents of the nitrene source (sPhINAr^{CF3} or sPhINAr^{NO2}) in anhydrous CH_2Cl_2 (0.1 mL) were added in that order to yield a deep purple intermediate. The formation of this species was monitored following the growth of the 525 nm band in the UV-Vis spectrum. **3-Sc**: UV-Vis (CH_2Cl_2, −90 °C): λ_{max} (ε_{max}, M^{-1} cm^{-1}): 525 nm (2150), 750 nm (600); **4-Sc**: UV-Vis (CH_2Cl_2, −90 °C): λ_{max} (ε_{max}, M^{-1} cm^{-1}): 525 nm (2000), 750 nm (550).

General procedure for the generation of 3 and 4: Under inert conditions, a colourless solution of the complex [(AN)Cu](BF$_4$) in anhydrous CH_2Cl_2 (1 mM, 2 mL) was cooled down to −90 °C. Then 1.5 equivalents of the nitrene source (sPhINAr^{CF3} or sPhINAr^{NO2}) in anhydrous CH_2Cl_2 (0.1 mL) were added with extreme precaution to avoid any oxygen or water getting in contact with the solution. The formation of a deep green intermediate was monitored following the growth of the 425 nm band in the UV-Vis spectrum. **3**: UV-Vis (CH_2Cl_2, −90 °C): λ_{max} (ε_{max}, M^{-1} cm^{-1}): 425 nm (1200), 700 nm (600); **4**: UV-Vis (CH_2Cl_2, −90 °C): λ_{max} (ε_{max}, M^{-1} cm^{-1}): 425 nm (1300), 700 nm (700).

Reactivity studies: A large excess of the respective substrate (> 20 eq) was dissolved in 0.1 mL of CH_2Cl_2 and added to 2 mL of a 1 mM solution of the preformed intermediate (**3**, **3-Sc**, **4** or **4-Sc**) at −90 °C. The decrease of the 425 or 525 nm band was monitored by UV-Vis spectroscopy and the obtained time trace fitted to a pseudo-first order decay curve. The second-order rate constants k_2 were obtained as the slope of the first-order rate constants k_{obs} vs the substrate concentration.

X-ray absorption spectroscopy: X-Ray absorption spectroscopy was carried out on the Stanford Synchrotron Radiation Lightsource (SSRL, Menlo Park, California) beamline (BL) 7–3 with SPEAR3 operating at 3 GeV and 500 mA in top-off mode throughout data collection. The BL 7–3 was equipped with a Rh coated collimating mirror followed by a cryogenically cooled Si(220) double crystal monochromator. The collimating mirror angle was set to 12 keV cutoffs for Cu K-edge measurements. Consequently, the monochromator was operated in the fully tuned configuration. Samples were kept at 10-15 K using an OXFORD LHE cryostat. XAS spectra were obtained with a "28" element solid-state germanium fluorescence detector (~20 working elements). A photodiode placed before I_0 and connected to I_2 was used to obtain a copper foil reference via scattering (reference is therefore I_0/I_2). Data was generally obtained on 0.95 mm x 4–6 mm (vertical x horizontal) spots. Scans were monitored for evidence of photoreduction, and new spots with fresh sample were exposed as needed. A 3 μ Z-1 filter and Soller slits were used to eliminate scatter, and ICR values typically ranged from 10–50 kcps. Data were collected with 10 eV steps before the edge (1 s integration time), 0.3 eV steps in pre-edge and edge regions (2 s integration time), and in 0.05k steps over $k = 1.62$ Å^{-1} to 14 or 15 Å^{-1} (integration time increased in k^2-weighted fashion from 2 to 9 sec over range of scan). Some scans were performed with XANES parameters, using a similar k-range but reducing integration times to 2–3 seconds in the EXAFS region. A 3.5 mM solution of [CuAN](BF4) was used to generate the intermediates for XAS analysis **4** and **4-Sc** with sPhINAr^{NO2} in the absence and in the presence of Sc(OTf)$_3$.

rRaman: rRaman spectra were measured at −90 °C (Bruker cryostat) with 532 nm excitation, by using a Horiba Jobin-Yvon LabRAM HR800 confocal Raman spectrometer. A 4 mM solution of [(AN)Cu](BF$_4$) was used to generate the intermediates **3-Sc** and **4-Sc** with sPhINAr^{CF3}, sPhINAr^{NO2} and their ^{15}N-labelled derivatives in the presence of Sc(OTf)$_3$.

Computational details: All DFT calculations were performed with the Amsterdam Density Functional (ADF) suite of program.[9] MOs were expanded in an uncontracted set of Slater type orbitals[10] (STOs) of triple- ζ quality containing diffuse functions and two sets of polarization functions (TZ2P), or a mixture of triple-ζ quality on the metal (TZP) and double-ζ quality (DZP) on all other atoms, in both cases with one set of polarization functions, which we dub here TDZP[10]. Core electrons (1s for 2nd period, 1s 2s 2p for 3rd–4th period) were not treated explicitly during the geometry optimizations (frozen core approximation), as it was shown to have a negligible effect on the obtained geometries.[11] An auxiliary set of s, p, d, f, and g STOs was used to fit the molecular density and to represent the Coulomb and exchange potentials accurately for each SCF cycle.

Geometries were optimized with the QUILD program[12] which uses superior optimization routines based on adapted delocalized coordinates[12] until the maximum gradient component was less than 10^{-4} a.u. This computational setup was shown to work well for transition-metal complexes.[13] The starting point for geometry optimizations were structures obtained from X-ray diffraction analysis. Energies and gradients were calculated using the BP86 functional[14] and the TDZP basis set with inclusion of Grimme's dispersion (D3) correction[15]. Subsequent single point calculations for obtaining spin-state splittings have been performed on all optimized geometries, with the S12 g functional[13] and the all-electron electron TZ2P basis set. The UV-Vis spectra were obtained in separate single-point calculations using the SAOP[16] model potential with the all-electron TZ2P basis set. In all cases the COSMO[17] dielectric continuum model has been included for implicit treatment of the environment (using dichloromethane as a solvent)[12,18], and scalar relativistic corrections have been included self-consistently by using the zeroth-order regular approximation (ZORA)[19]. All computational data are uploaded (DOI:10.19061/iochem-bd-4-28) onto the IOCHEM-BD platform (www.iochem-

bd.org) to facilitate data exchange and dissemination, according to the FAIR principles[22] of OpenData sharing.

Acknowledgements

The following organizations are thanked for financial support: the Ministerio de Ciencia e Innovación (MICINN, project CTQ2011-25086/BQU), the Ministerio de Economia y Competitividad (MINECO, projects CTQ2014-59212-P and CTQ2015-70851-ERC) and the Generalitat de Catalunya (project 2014SGR1202, and Xarxa de Referència en Química Teòrica i Computacional). Financial support was provided by MICINN and the FEDER funds (European Fund for Regional Development) under grant UNGI10-4E-801. We also gratefully acknowledge financial support of this work from the Deutsche Forschungsgemeinschaft (DFG, German Research Foundation) under Germany's Excellence Strategy – EXC 2008 – 390540038 – UniSysCat/"Unifying Concepts in Catalysis" (EXC 314/1), Berlin. IMP thanks BIG-NSE for a scholarship. K. W. thanks Einstein Foundation Berlin (ESB) – Einstein Center of Catalysis (EC^2) for its support. This work was performed in the framework of the COST action CM1305 "Explicit Control Over Spin-states in Technology and Biochemistry (ECOSTBio)". XAS measurements on SSRL beamline 7-3 benefited from support of SSRL by the US DOE Office of Science, Office of Basic Energy Sciences, under Contract No. DE-AC02-76SF00515 and support of the SSRL Structural Molecular Biology Program by the DOE Office of Biological and Environmental Research and NIH NIGMS (P30GM133894). Open access funding enabled and organized by Projekt DEAL.

Keywords: Copper Nitrene · High-Valent Copper · Hydrogen Atom Transfer · Aziridination · Density Functional Theoretical Calculations

[1] C. E. Elwell, N. L. Gagnon, B. D. Neisen, D. Dhar, A. D. Spaeth, G. M. Yee, W. B. Tolman, *Chem. Rev.* **2017**, *117*, 2059–2107.

[2] a) N. Dietl, C. van der Linde, M. Schlangen, M. K. Beyer, H. Schwarz, *Angew. Chem. Int. Ed.* **2011**, *50*, 4966–4969; *Angew. Chem.* **2011**, *123*, 5068–5072; b) D. Schröder, M. C. Holthausen, H. Schwarz, *J. Phys. Chem. B* **2004**, *108*, 14407–14416; c) D. Schröder, H. Schwarz, *Angew. Chem. Int. Ed. Engl.* **1995**, *34*, 1973–1995; d) M. Srnec, R. Navrátil, E. Andris, J. Jašík, J. Roithová, *Angew. Chem. Int. Ed.* **2018**, *57*, 17053–17057; *Angew. Chem.* **2018**, *130*, 17299–17303; e) G. Yassaghi, E. Andris, J. Roithová, *ChemPhysChem* **2017**, *18*, 2217–2224; f) L. Jašíková, E. Hanikýřová, D. Schröder, J. Roithová, *J. Mass Spectrom.* **2012**, *47*, 460–465.

[3] a) Y. M. Badiei, A. Krishnaswamy, M. M. Melzer, T. H. Warren, *J. Am. Chem. Soc.* **2006**, *128*, 15056–15057; b) M. J. B. Aguila, Y. M. Badiei, T. H. Warren, *J. Am. Chem. Soc.* **2013**, *135*, 9399–9406; c) F. Dielmann, D. M. Andrada, G. Frenking, G. Bertrand, *J. Am. Chem. Soc.* **2014**, *136*, 3800–3802; d) I. Monte-Pérez, S. Kundu, K. Ray, *Z. Anorg. Allg. Chem.* **2015**, *641*, 78–82; e) S. Kundu, E. Miceli, E. Farquhar, F. F. Pfaff, U. Kuhlmann, P. Hildebrandt, B. Braun, C. Greco, K. Ray, *J. Am. Chem. Soc.* **2012**, *134*, 14710–14713; f) S.-L. Abram, I. Monte-Pérez, F. F. Pfaff, E. R. Farquhar, K. Ray, *Chem. Commun.* **2014**, *50*, 9852–9854; g) T. Corona, L. Ribas, M. Rovira, E. R. Farquhar, X. Ribas, K. Ray, A. Company, *Angew. Chem. Int. Ed.* **2016**, *55*, 14005–14008; *Angew. Chem.* **2016**, *128*, 14211–14214; h) J. Moegling, A. Hoffmann, F. Thomas, N. Orth, P. Liebhäuser, U. Herber, R. Rampmaier, J. Stanek, G. Fink, I. Ivanović-Burmazović, S. Herres-Pawlis, *Angew. Chem. Int. Ed.* **2018**, *57*, 9154–9159; *Angew. Chem.* **2018**, *130*, 9294–9299; i) K. M. Carsch, I. M. DiMucci, D. A. Iovan, A. Li, S.-L. Zheng, C. J. Titus, S. J. Lee, K. D. Irwin, D. Nordlund, K. M. Lancaster, T. A. Betley, *Science* **2019**, *365*, 1138–1143; j) N. R. M. de Kler, J. Roithová, *Chem. Commun.* **2020**, *56*, 12721–12724.

[4] a) S. Hong, F. F. Pfaff, E. Kwon, Y. Wang, M.-S. Seo, E. Bill, K. Ray, W. Nam, *Angew. Chem. Int. Ed.* **2014**, *53*, 10403–10407; *Angew. Chem.* **2014**, *126*, 10571–10575; b) F. F. Pfaff, S. Kundu, M. Risch, S. Pandian, F. Heims, I. Pryjomska-Ray, P. Haack, R. Metzinger, E. Bill, H. Dau, P. Comba, K. Ray, *Angew. Chem. Int. Ed.* **2011**, *50*, 1711–1715; *Angew. Chem.* **2011**, *123*, 1749–1753; c) S. Fukuzumi, Y. Morimoto, H. Kotani, P. Naumov, Y.-M. Lee, W. Nam, *Nat. Chem.* **2010**, *2*, 756–759; d) F. F. Pfaff, F. Heims, S. Kundu, S. Mebs, K. Ray, *Chem. Commun.* **2012**, *48*, 3730–3732.

[5] a) H. Kwart, A. A. Kahn, *J. Am. Chem. Soc.* **1967**, *89*, 1950–1951; b) P. Müller, C. Fruit, *Chem. Rev.* **2003**, *103*, 2905–2920; c) M. R. Fructos, S. Trofimenko, M. M. Díaz-Requejo, P. J. Pérez, *J. Am. Chem. Soc.* **2006**, *128*, 11784–11791; d) M. M. Díaz-Requejo, T. R. Belderraín, M. C. Nicasio, S. Trofimenko, P. J. Pérez, *J. Am. Chem. Soc.* **2003**, *125*, 12078–12079; e) M. M. Díaz-Requejo, P. J. Pérez, M. Brookhart, J. L. Templeton, *Organometallics* **1997**, *16*, 4399–4402; f) Y. M. Badiei, A. Dinescu, X. Dai, R. M. Palomino, F. W. Heinemann, T. R. Cundari, T. H. Warren, *Angew. Chem. Int. Ed.* **2008**, *47*, 9961–9964; *Angew. Chem.* **2008**, *120*, 10109–10112; g) Z. Li, R. W. Quan, E. N. Jacobsen, *J. Am. Chem. Soc.* **1995**, *117*, 5889–5890.

[6] a) E. J. Klinker, S. Shaik, H. Hirao, L. Que Jr., *Angew. Chem. Int. Ed.* **2009**, *48*, 1291–1295; *Angew. Chem.* **2009**, *121*, 1317–1321; b) S. Shaik, H. Hirao, D. Kumar, *Acc. Chem. Res.* **2007**, *40*, 532–542; c) H. Hirao, D. Kumar, L. Que, S. Shaik, *J. Am. Chem. Soc.* **2006**, *128*, 8590–8606.

[7] A singlet Cu(I) electronic structure was obtained from DFT calculations which is consistent with the electronic absorption spectra at −90 °C in dichloromethane, however not consistent from XAS studies at 4 K. Whether a temperature-dependent redox tautomerization is present is now an interesting question which will be investigated in future studies.

[8] D. Macikenas, E. Skrzypczak-Jankun, J. D. Protasiewicz, *J. Am. Chem. Soc.* **1999**, *121*, 7164–7165.

[9] a) E. J. Baerends, J. Autschbach, A. Bérces, J. A. Berger, F. M. Bickelhaupt, C. Bo, P. L. de Boeij, P. M. Boerrigter, L. Cavallo, D. P. Chong, L. Deng, R. M. Dickson, D. E. Ellis, M. van Faassen, L. Fan, T. H. Fischer, C. Fonseca Guerra, S. J. A. van Gisbergen, J. A. Groeneveld, O. V. Gritsenko, M. Grüning, F. E. Harris, P. van den Hoek, C. R. Jacob, H. Jacobsen, L. Jensen, E. S. Kadantsev, G. van Kessel, R. Klooster, F. Kootstra, E. van Lenthe, D. A. McCormack, A. Michalak, J. Neugebauer, V. P. Nicu, V. P. Osinga, S. Patchkovskii, P. H. T. Philipsen, D. Post, C. C. Pye, W. Ravenek, P. Romaniello, P. Ros, P. R. T. Schipper, G. Schreckenbach, J. G. Snijders, M. Solà, M. Swart, D. Swerhone, G. te Velde, P. Vernooijs, L. Versluis, L. Visscher, O. Visser, F. Wang, T. A. Wesolowski, E. M. van Wezenbeek, G. Wiesenekker, S. K. Wolff, T. K. Woo, A. L. Yakovlev, T. Ziegler, 2013.01 ed., SCM, Amsterdam, **2013**, p. ADF; b) G. te Velde, F. M. Bickelhaupt, E. J. Baerends, C. Fonseca Guerra, S. J. A. van Gisbergen, J. G. Snijders, T. Ziegler, *J. Comput. Chem.* **2001**, *22*, 931–967.

[10] D. P. Chong, E. Van Lenthe, S. Van Gisbergen, E. J. Baerends, *J. Comput. Chem.* **2004**, *25*, 1030–1036.

[11] M. Swart, J. G. Snijders, *Theor. Chem. Acc.* **2003**, *110*, 34–41, Erratum: ibid 111, 156.

[12] M. Swart, F. M. Bickelhaupt, *J. Comput. Chem.* **2008**, *29*, 724–734.
[13] M. Swart, *Chem. Phys. Lett.* **2013**, *580*, 166–171.
[14] a) J. P. Perdew, *Phys. Rev. B* **1986**, *33*, 8822–8824; b) A. D. Becke, *J. Chem. Phys.* **1988**, *88*, 2547–2553.
[15] S. Grimme, J. Antony, S. Ehrlich, H. Krieg, *J. Chem. Phys.* **2010**, *132*, 154104.
[16] P. R. T. Schipper, O. V. Gritsenko, S. J. A. van Gisbergen, E. J. Baerends, *J. Chem. Phys.* **2000**, *112*, 1344–1352.
[17] a) A. Klamt, V. Jonas, *J. Chem. Phys.* **1996**, *105*, 9972–9981; b) A. Klamt, *J. Phys. Chem.* **1995**, *99*, 2224–2235; c) A. Klamt, G. Schüürmann, *J. Chem. Soc. Perkin Trans. 2* **1993**, 799–805.
[18] C. C. Pye, T. Ziegler, *Theor. Chem. Acc.* **1999**, *101*, 396–408.
[19] a) E. van Lenthe, A. Ehlers, E.-J. Baerends, *J. Chem. Phys.* **1999**, *110*, 8943–8953; b) E. van Lenthe, E. J. Baerends, J. G. Snijders, *J. Chem. Phys.* **1994**, *101*, 9783–9792; c) E. v. Lenthe, E. J. Baerends, J. G. Snijders, *J. Chem. Phys.* **1993**, *99*, 4597–4610.

Manuscript received: March 15, 2021
Revised manuscript received: April 30, 2021
Accepted manuscript online: May 16, 2021

